RFID MEMS Sensor Concept Based on Intermodulation Distortion

Ville Viikari, *Member, IEEE*, and Heikki Seppä

***Abstract*—This paper presents a passive wireless microelectromechanical systems (MEMS) sensor consisting of an antenna directly matched to a MEMS resonator. When the sensor is actuated at two signals at different frequencies it replies at an intermodulation frequency. An analytical equation for the mixing efficiency of a MEMS sensor is derived and verified by harmonic balance simulations. The concept is demonstrated experimentally and shown to be feasible for implementing sensors or tags readable across large distances.**

***Index Terms*—Mixers, radio frequency (RF) microelectromechanical systems (MEMS), radio frequency identification (RFID), wireless sensors.**

I. Introduction

Wireless sensors have a great deal of potential in numerous applications that are too expensive or impossible to monitor by wire. Wireless sensors are divided into battery-powered active devices containing a radio transmitter, semi-passive battery-assisted sensors using modulated backscattering technique, and fully passive sensors. The disadvantages of active sensors are their high cost and limitations due to the battery's lifetime. Existing passive and semi-passive wireless sensors are based either on silicon-based radio frequency identification (RFID) or surface acoustic wave (SAW) technology.

Advanced RFID technology enables low-cost passive and semi-passive tags (i.e., ID-sensors) with rewritable memory. The technology can be used to realize general sensor platform [1], and it has been used to implement for example temperature [2] and shock [3] sensors. The RFID technology has some drawbacks in sensor applications. The power rectifier that generates the required power for the IC limits both the highest operation frequency and the largest distance. Therefore, passive RFID tags are not feasible in applications where a high operation frequency or a large interrogation distance is required. High frequency enables the small antenna size and precise spatial localization of the tag.

SAW tags offer several advantages when used as a sensor: they are small, withstand harsh environment, enable a relatively long reading distance, are passive, and are inherently sensitive to some quantities without external sensor elements [4]. A disadvantage with SAW sensors is that they are expensive compared to silicon-based sensors due to higher prices of piezoelectric substrates. In addition, the highest operation frequency of a SAW sensor is limited by the line width of the metal pattern printed on the piezoelectric substrate and it is typically a few GHz.

This paper presents a passive wireless sensor or tag that can be implemented with the well-established MEMS technology. This wireless MEMS sensor enables very low manufacturing costs, long reading distance, high frequencies, and compact tag size. In addition, the wireless sensors can be passive requiring no embedded electronics.

This wireless sensor, when illuminated at two harmonic frequencies, produces an intermodulation frequency, which is emitted to the reader. The interrogation method of the proposed sensor is somewhat similar to the harmonic radar concept, which was first proposed for traffic applications [5] and later was used for tracking insects [6]–[8]. However, as compared to the harmonic radar, the proposed method enables a smaller frequency offset between the transmitted and received signals which eases to fulfill the frequency regulations and facilitates circuit design. The interrogation method is proposed for automotive radars to detect pedestrians, bicyclists, and other road users who are high risk to serious injury in traffic accidents [9].

The intermodulation distortion of MEMS devices have been studied in several articles. The intermodulation distortion in capacitive MEMS switches is approximated in [10] and [11]. These models assume small MEMS cantilever displacement and high bridge impedance and neglect the mechanical quality factor of the MEMS. More comprehensive analysis presented in [12] takes also fifth-order nonlinearities into account. Another approach based on Volterra-series is presented in [13]. An analytical model for intermodulation distortion due to contact heating in contacting MEMS switches is presented in [14]. In addition, the MEMS mixer-filters [15]–[18], also called mixlers, share somewhat similar operating principle to the proposed MEMS sensor.

The proposed MEMS device uses an electrical matching circuit and potentially very high mechanical quality factor of the MEMS to maximize the intermodulation distortion. These phenomena are neglected in the models presented in [10] and [11], while the complex models presented in [12] and [13] are unpractical for the purpose of this paper. Section II derives a simple but comprehensive model for the intermodulation response of the MEMS device.

Manuscript received April 23, 2009; revised July 31, 2009; accepted September 01, 2009. Current version published October 28, 2009. This work was supported in part by the EU Commission under the Contract FP7-ICT-2007-1-216049 of the ADOSE Project. The associate editor coordinating the review of this paper and approving it for publication was Prof. Okyay Kaynak.

The authors are with the VTT Technical Research Centre, Tietotie 3, Espoo, Finland, (e-mail: ville.viikari@vtt.fi, heikki.seppa@vtt.fi).

Color versions of one or more of the figures in this paper are available online at http://ieeexplore.ieee.org.

Digital Object Identifier 10.1109/JSEN.2009.2031809

1530-437X/$26.00 © 2009 IEEE

Authorized licensed use limited to: Valtion Teknillinen Tutkimuskeskus. Downloaded on November 26, 2009 at 05:25 from IEEE Xplore. Restrictions apply.

II. Theory of the Intermodulating Sensor

A. Dynamic Response of Cantilever

Let us consider an electrostatically actuated MEMS cantilever or fixed–fixed beam structure as a mass-spring system. Assuming that the beam vibrates only in one mode (typically the lowest order mode), its dynamic response is given as [19]

$$m\frac{d^2}{dt^2}x+\eta\frac{d}{dt}x+kx=F \tag{1}$$

where m is the effective mass of the cantilever, x is the cantilever displacement, η is the damping coefficient, k is the effective spring constant and F is the external force affecting the cantilever. The amplitude of the vibration is given for harmonic force as [19]

$$\hat{x}=\frac{\hat{F}_\omega Q_m}{k}g_n\left(\omega,\omega_m,Q_m\right) \tag{2}$$

where $\hat{F}_\omega$ is the amplitude of the harmonic force at the frequency ω, $Q_m=\omega_m m/\eta$ is the mechanical quality factor of the resonator, and g_n is the normalized frequency response given as

$$g_n\left(\omega,\omega_m,Q_m\right)=\frac{\omega_m}{\omega\sqrt{1+\left(\frac{Q_m\left(\omega^2-\omega_m^2\right)}{\omega\omega_m}\right)^2}} \tag{3}$$

where ω_m is the mechanical resonance frequency of the cantilever. Considering the cantilever as an air-filled parallel-plate capacitor and assuming that a voltage V is applied over the capacitance, the electrical force is given as

$$F=-\frac{d}{dx}\frac{V^2\varepsilon_0 A}{2\left(g_0-x\right)}\approx\frac{C_0V^2}{2g_0} \tag{4}$$

where ε_0 is the permittivity of vacuum, A is the capacitor area, g_0 is the initial gap height of the capacitor, and $C_0=\varepsilon_0 A/g_0$ is the initial capacitance. The displacement is assumed to be small (compared to g_0) in the first order Taylor approximation. When the cantilever is actuated with the voltage V consisting of two sinusoids, $\hat{V}_1\sin\omega_1 t$ and $\hat{V}_2\sin\omega_2 t$, the force contains four harmonic terms and is given as

$$F\left(t\right)\approx\frac{C_0}{2g_0}\left\{\frac{\hat{V}_1^2+\hat{V}_2^2}{2}+\hat{V}_1\hat{V}_2\cos\left(\omega_2-\omega_1\right)t\right.$$
$$\left.-\hat{V}_1\hat{V}_2\cos\left(\omega_2+\omega_1\right)t-\frac{\hat{V}_1^2}{2}\cos 2\omega_1 t-\frac{\hat{V}_2^2}{2}\cos 2\omega_2 t\right\}. \tag{5}$$

Let us assume that the cantilever is grounded at DC and that the angular frequencies ω_1 and ω_2 are well above the mechanical resonance frequency ω_m of the cantilever mass-spring system. Then, the DC and high-frequency force terms can be neglected and the amplitude of the vibration in (2) can be written as

$$\hat{x}=\frac{C_0\hat{V}_1\hat{V}_2Q_m}{2kg_0}g_n\left(\omega_\Delta,\omega_m,Q_m\right) \tag{6}$$

where $\omega_\Delta=\omega_2-\omega_1$.

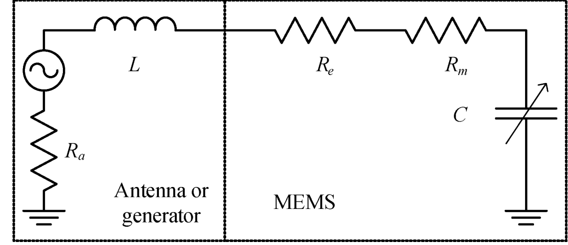

Fig. 1. The equivalent circuit of MEMS resonator matched to an antenna or generator.

B. Mixing Efficiency of MEMS

Consider a MEMS resonator that is conjugate matched ($L=1/(\omega^2C_0)$ and $R_a=R_m+R_e$) to an antenna or equivalently a generator, as shown in Fig. 1. The resistance R_e denotes the conductor losses and R_m the mechanical power dissipation due to friction.

The antenna receives powers P_1 and P_2 at frequencies ω_1 and ω_2, respectively, producing peak voltages $\hat{V}_1=\sqrt{2P_2R_a}$ and $\hat{V}_2=\sqrt{2P_2R_a}$. Substituting the voltages into (6) gives

$$x\left(t\right)=\frac{C_0R_a\sqrt{P_1P_2}Q_m}{kg_0}g_n\left(\omega_\Delta,\omega_m,Q_m\right)\sin\omega_\Delta t. \tag{7}$$

The movement of the cantilever modulates the capacitance, which can be approximated, when the movement is small, as

$$C\approx\frac{C_0}{g_0}x=\frac{C_0^2R_a\sqrt{P_1P_2}Q}{kg_0^2}g_n\left(\omega_\Delta,\omega_m,Q_m\right)\sin\omega_\Delta t. \tag{8}$$

When the matching inductance of the equivalent circuit of MEMS resonator is $L=1/\left(\omega^2C_0\right)$, the reflection coefficient of the circuit is given as

$$\Gamma=\frac{-j\omega\Delta C}{\frac{2}{R_a}+j\omega\Delta C}\approx\frac{j\omega R_a\Delta C}{2} \tag{9}$$

where $\Delta C=C-C_0$. The reflection coefficient oscillates at the frequency of ω_m, and therefore harmonically modulates the applied signal. The ratio between the modulated power at one side band and the received power at one frequency, the conversion efficiency is

$$\left|\frac{\Delta\Gamma}{2}\right|^2=\left(\frac{Q_e^2\sqrt{P_1P_2}Q_m}{4\omega_e kg_0^2}g_n\left(\omega_\Delta,\omega_m,Q_m\right)\right)^2 \tag{10}$$

where the electrical quality factor $Q_e=\omega RC_0$ is given as for parallel resonance circuit.

C. Equivalent Resistance of the MEMS

The above analysis showed that the conversion efficiency is proportional to the fourth power of the electrical quality factor if the electrical resonance circuit is in resonance at both fundamental frequencies f_1 and f_2, the electrical bandwidth of the resonator circuit is larger than the mechanical resonance frequency ($\omega_e/Q_e>\omega_m$). The electrical quality factor is limited either by the conductor losses or by the equivalent electrical resistance of the MEMS resonator. Let us next calculate the equivalent electrical resistance due to friction neglecting conductor

Authorized licensed use limited to: Valtion Teknillinen Tutkimuskeskus. Downloaded on November 26, 2009 at 05:25 from IEEE Xplore. Restrictions apply.

losses. The equivalent resistance of the MEMS is calculated under conjugate matching, as the highest conversion efficiency occurs in that point. The electrical dissipations must equal to the mechanical power loss in the MEMS resonator, which is given as

$$P_{mech} = \frac{\omega_r}{Q}\frac{1}{2}k\hat{x}^2. \tag{11}$$

Substituting (6) into (11), assuming that $P_1 = P_2$ and setting mechanical power loss equal to the electrical losses at both frequencies gives

$$R_a = \sqrt{\frac{4kg_0^2}{\omega_r C_0^2 P Q_m}}. \tag{12}$$

The loss tangent of the MEMS capacitor is given as

$$\tan\delta = \sqrt{\frac{\omega_r P Q_m}{4kg_0^2\omega_e^2}}. \tag{13}$$

The previous analysis neglected the modulation reflection coefficient which increases in the fourth power of R_a (in parallel circuit) and decreases the power matched to the equivalent resistance of the MEMS. Therefore, this analysis underestimates the equivalent resistance. However, (13) shows that the loss tangent of the MEMS resonator is typically very low at low input power levels, and therefore the loss tangent of a practical system is dominated by conductor losses. For example, the equivalent loss tangent of a resonator with $k = 11$ N/m, $g_0 = 1.2\ \mu$m, $f_r = 127$ kHz, $P = -40$ dBm, and $Q_m = 250$ is $9 \cdot 10^{-5}$ at 1 GHz.

III. Experiments and Simulations

A. Measured MEMS Device

A capacitive RF MEMS switch was used to experimentally verify the concept. The MEMS switch was bond wired to a grounded coplanar waveguide. A lumped inductor of 36 nH ($Q = 100$ at 1 GHz) was soldered in series with the switch in order to obtain electrical matching. The zero voltage capacitance and the pull-in voltages were measured to be 190 fF and 5 V, respectively. The initial gap height was designed to be 1.2 μm and the mechanical resonance of the switch was found to occur at around 127 kHz. The unpacked MEMS device was kept in vacuum (~ 1 mBar) during the tests in order to increase its mechanical quality factor, which was below one at atmospheric pressure. A high-quality factor could also be achieved by using hermetically packed MEMS component.

B. Measurement Setup

A schematic layout of the measurement setup is shown in Fig. 2. Both tones were generated with signal generators (Agilent E8257C and E8257D), combined in power combiner and fed to the MEMS device through a circulator. The generators were isolated to prevent intermodulation in the generators. The reflected signal at an intermodulation frequency was separated with the circulator and measured with spectrum analyzer (Rohde & Schwarz FSP). The nominal frequency range of the isolators and circulator is from 1 to 2 GHz, which was slightly exceeded in the experiments. An attenuator was used in front of the spectrum analyzer in order to suppress the third-order harmonics generated in the mixer of the spectrum analyzer. The signal generators and the spectrum analyzer were controlled with a LabVIEW[1]-based software. A photograph of the measurement setup is shown in Fig. 3.

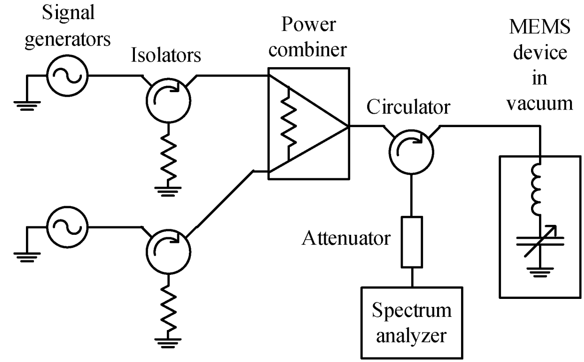

Fig. 2. A schematic layout of the measurement setup for measuring the reflected intermodulation signal from the MEMS device.

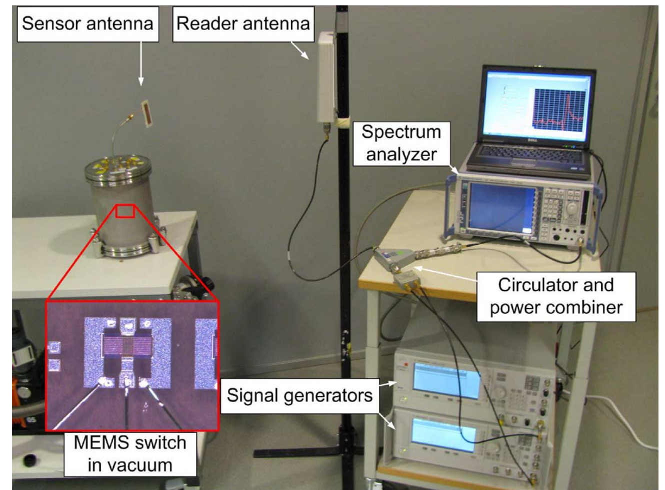

Fig. 3. The measurement setup for measuring the reflected signal from the MEMS device at an intermodulation frequency. The setup in the photograph is wireless even though the measurements presented in this paper are made by wired connection.

C. Simulated MEMS Device

The purpose of the simulations is to verify the theoretical results and, therefore, the simulated circuit is equal to that presented in Fig. 1. The initial capacitance, the gap height and the spring constant of the simulated MEMS are equal to those of the experimental device. The spring constant of the switch was calculated from

$$k = \frac{27V_{pi}^2 C_0}{8g_0^2} \tag{14}$$

and it was found to be $k = 11$ N/m ($V_{pi} = 5$ V is the measured pull-in voltage). The electrical and mechanical quality factors as well as resonance frequencies are selected by fitting the simulated results to the measured ones. Note that the experimental

[1]http://www.ni.com/labview/

Authorized licensed use limited to: Valtion Teknillinen Tutkimuskeskus. Downloaded on November 26, 2009 at 05:25 from IEEE Xplore. Restrictions apply.

TABLE I
THE PARAMETERS OF THE MEMS USED IN SIMULATIONS AND CALCULATIONS

Zero voltage capacitance	$C_0 = 190$ fF
Gap height	$g_0 = 1.2\ \mu$m
Spring constant	$k = 11$ N/m
Mechanical resonance frequency*	$f_m = 126.75$ kHz
Electrical resonance frequency*	$f_e = 950$ MHz
Mechanical quality factor*	$Q_m = 250$
Electrical quality factor*	$Q_e = 4$
Series resistance of generator and MEMS	$R = 220\ \Omega$
Series matching inductance	$L = 147.7$ nH

*Fitted to the measurements.

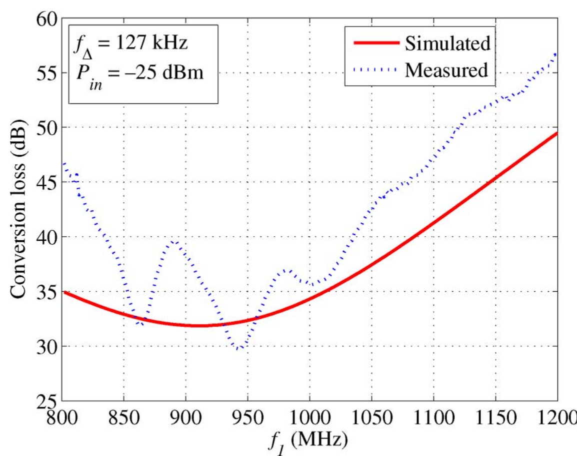

Fig. 4. The measured and simulated conversion losses of the MEMS device. The frequency difference is 127 kHz and the input power level -25 dBm.

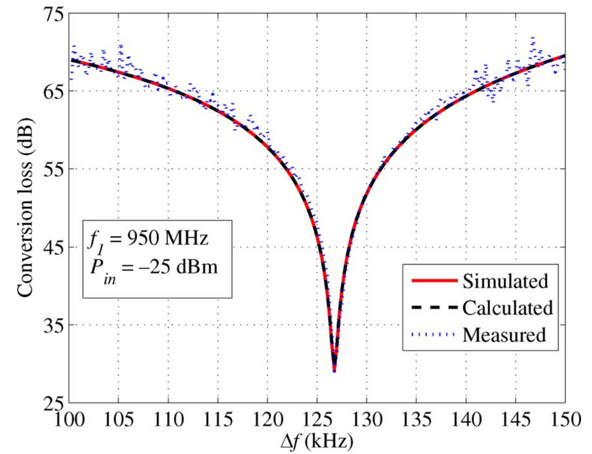

Fig. 5. The measured, simulated, and calculated conversion loss of the MEMS device as a function of the input frequency difference. The constant frequency is 950 MHz and the input power level is -25 dBm.

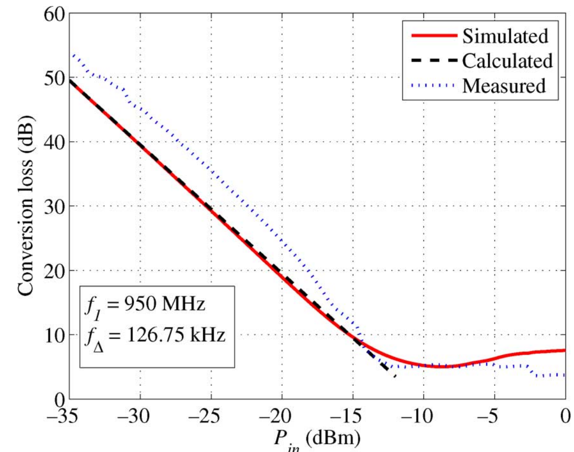

Fig. 6. The conversion loss of the MEMS device as a function of the input power level.

device may suffer from impedance mismatch between the generator and the MEMS, which is included into electrical quality factor in the fitting process. The parameters of the simulated device are listed in Table I. These parameters are also used in analytically calculated curves.

The electrical response of the system, including electrical circuit and the MEMS switch, is simulated with Aplac[2]-software using harmonic balance analysis.

D. Results

The realized electrical center frequency of the MEMS device was studied by sweeping both input frequencies, keeping the frequency difference constant, and recording the reflected signal at an intermodulation frequency. Fig. 4 shows the measured and simulated conversion loss as a function of electrical input frequency when the input power is -25 dBm and the frequency difference is 127 kHz.

Fig. 4 shows that the best electrical matching of the experimental device occurs at around 950 MHz. The measured curve introduces strong and fast varying ripple that does not exist in the simulated curve. The nominal frequency range of the isolators and circulator (1–2 GHz) was slightly exceeded and the ripple may therefore derive from multiple reflections in the feeding network. However, the overall trend of the measured curve corresponds well to the simulated one.

The mechanical resonance of the device was studied by fixing one of the input frequencies and sweeping another. Fig. 5 shows the measured, simulated, and calculated conversion losses as a function of the frequency difference at -25 dBm input power level. The simulated and calculated curves are perfectly aligned and that the measured curve correspond very well to these. Note that small deviation at high conversion loss values is due to low signal-to-noise-ratio in the measurements.

Fig. 6 shows the measured, simulated, and calculated conversion losses of the MEMS device at different input power levels. The lower input frequency is 950 MHz and the frequency difference 126.75 kHz. Fig. 6 exhibits a good agreement between the simulated and calculated curves at small power levels. The analytically calculated curve would naturally fail at high-power levels as small cantilever movement was assumed in the derivation. The measured curve introduces approximately 5 dB larger conversion loss as compared to simulations and calculations at small power levels (< -17 dBm). The mechanical resonance frequency of the switch was found to drift during the experiments and we assume that the 5 dB deviation between the measured and simulated curves occurs because the switch is not excited exactly at its nominal frequency.

[2]http://web.awrcorp.com/

Authorized licensed use limited to: Valtion Teknillinen Tutkimuskeskus. Downloaded on November 26, 2009 at 05:25 from IEEE Xplore. Restrictions apply.

TABLE II
THE CALCULATED LINK BUDGET OF A WIRELESS MEMS SENSOR INTERROGATED WITH A READER DEVICE

Transmitted power	$P_t = 20$ dBm
Reader antenna gain	$G_{reader} = 10$ dBi
Free space loss	$\left(\frac{\lambda}{4\pi r}\right)^2 = -67$ dB
Sensor antenna gain	$G_{sensor} = 0$ dBi
Received power by the sensor	$P_{sensor} = -37$ dBm
Intermodulation mixing loss	$L = -10$ dB
Sensor antenna gain	$G_{sensor} = 0$ dBi
Free space loss	$\left(\frac{\lambda}{4\pi r}\right)^2 = -67$ dB
Reader antenna gain	$G_{reader} = 10$ dBi
Received power at intermodulation frequency	$P_r = -104$ dBm

IV. UTILIZATION AS TAG OR SENSOR

A. Detection Distance

The intermodulation conversion efficiency given in (10) of the proposed MEMS device can be tailored to be extremely low by increasing the electrical and mechanical quality factors and decreasing the mechanical resonance frequency and the mechanical spring constant. Therefore, the detection distance of such MEMS sensor is not limited by the conversion loss. For example, considering a MEMS resonator with $Q_e = 40$ and otherwise being similar to that used in the experiments, the conversion loss is 47 dB smaller than that of the experimental device enabling efficient mixing (10 dB mixing loss) at $-37\ \mathrm{dBm}$ input power. Such a device provides approximately 60 m detection distance at 870 MHz RFID-band assuming transmitted power of 20 dBm at one frequency (33 dBm ERP allowed for RFID readers), transmitter antenna gain of 10 dBi, a sensor antenna gain of 0 dB, and a receiver sensitivity of $-104\ \mathrm{dBm}$. The corresponding link budget calculation is presented in Table II. The detection distance of the prototype sensor with $Q_e = 4$ is 17 m.

B. Wireless Sensor

The presented concept allows wirelessly measuring three MEMS parameters: the mechanical quality factor, the mechanical resonance frequency, and the electrical resonance frequency. Two former parameters are measured by sweeping one of the input frequencies and keeping the other fixed, whereas the latter is obtained by sweeping both input frequencies at the same rate.

The wireless sensor can be implemented by designing the MEMS resonator as such that at least one of the three parameters is sensitive to the measured quantity, such as temperature, strain, air pressure or humidity. For example, MEMS fixed–fixed beam structure could be designed such that the beam is either stressed or compressed due to change in temperature or strain. The stress affects the spring constant of the beam changing the mechanical resonance frequency. This interrogation method with wire is used for example for monitoring the mechanical stress in RF MEMS capacitive switches [20].

Similarly, friction of the unpacked cantilever structure is related to the mechanical quality factor and is sensitive to air pressure and humidity. The third possibility is to determine the measured quantity from the electrical resonance frequency. For instance, consider a MEMS pressure sensor with cavity backed membrane. The ambient pressure depresses the membrane affecting the gap height and the initial capacitance. Changed capacitance shifts the electrical resonance of the *LC*-circuit.

V. CONCLUSION

We have presented a principle for a novel wireless MEMS sensor. The sensor, when illuminated with two signals at different frequencies, emits the sensor data to the reader at one of the intermodulation frequencies. In this paper, we have derived an analytical equation describing the mixing efficiency of such a sensor at low-power levels, which can be used to predict the achievable detection distance. The performance of the MEMS sensor is also simulated and the excellent agreement with the analytical and simulated results verifies the theory. The concept is experimentally demonstrated by using a capacitive MEMS switch in vacuum as a resonator. The resonator is bond wired to a coplanar waveguide and matched with a lumped inductor for 950 MHz frequency. The experimental results validate the feasibility of the concept.

REFERENCES

[1] A. P. Sample, D. J. Yeager, P. S. Powledge, A. V. Mamishev, and J. R. Smith, "Design of an RFID-based battery-free programmable sensing platform," *IEEE Trans. Instrum. Measure.*, vol. 57, pp. 2608–2615, Nov. 2008.

[2] K. Opasjumruskit, T. Thanthipwan, O. Sathusen, P. Sirinamarattana, P. Gadmanee, E. Pootarapan, N. Wongkomet, A. Thanachayanont, and M. Thamsirianunt, "Self-powered wireless temperature sensors exploit RFID technology," *IEEE Pervasive Comput.*, vol. 5, no. 1, pp. 54–61, Jan.–Mar. 2006.

[3] B. Todd, M. Phillips, S. M. Schultz, A. R. Hawkins, and B. D. Jensen, "Low-cost RFID threshold shock sensors," *IEEE Sensors J.*, vol. 9, pp. 464–469, Apr. 2009.

[4] L. Reindl, G. Scholl, T. Ostertag, H. Scherr, U. Wolff, and F. Schmidt, "Theory and application of passive SAW radio transponders as sensors," *IEEE Trans. Ultrason., Ferroelectr. Freq, Control*, vol. 45, pp. 1281–1292, Sep. 1998.

[5] H. Staras and J. Shefer, "Harmonic radar detecting and ranging system for automotive vehicles," U.S. Patent 3781879, 1972.

[6] E. T. Cant, A. D. Smith, D. R. Reynold, and J. L. Osborne, "Tracing butterfly flight paths across the landscape with harmonic radar," in *Proc. Royal Soc. B: Bio. Sci.*, Apr. 2005, vol. 272, pp. 785–790, 1565.

[7] J. R. Riley and A. D. Smith, "Design considerations for an harmonic radar to investigate the flight of insects at low altitude," in *Computers and Electronics in Agriculture*. Amsterdam, The Netherlands: Elsevier, 2002, vol. 35, pp. 151–169.

[8] B. G. Colpitts and G. Boiteau, "Harmonic radar transceiver design: Miniature tags for insect tracking," *IEEE Trans. Antennas Propag.*, vol. 52, pp. 2825–2832, Nov. 2004.

[9] V. Viikari, J. Saebboe, S. Cheng, M. Kantanen, M. Al-Nuaimi, T. Varpula, A. Lamminen, P. Hallbjörner, A. Alastalo, T. Mattila, H. Seppä, P. Pursula, and A. Rydberg, "Technical solutions for automotive intermodulation radar for detecting vulnerable road users," in *Proc. IEEE 69th Veh. Technol. Conf.*, Barcelona, Spain, Apr. 26 – 29, 2009.

[10] L. Dussopt and G. M. Rebeiz, "Intermodulation distortion and power handling in FR MEMS switches, varactors, and tunable filters," *IEEE Trans. Microw. Theory Tech.*, vol. 51, pp. 1247–1256, Apr. 2003.

[11] P. Hallbjörner and P. J. Starski, "Expressions for nonlinear effects of MEMS switch beam oscillations," *IEE Electron. Lett.*, vol. 37, no. 11, pp. 693–694, May 2001.

Authorized licensed use limited to: Valtion Teknillinen Tutkimuskeskus. Downloaded on November 26, 2009 at 05:25 from IEEE Xplore. Restrictions apply.

[12] D. Girbau, N. Otegi, L. Pradell, and A. Lazaro, "Study of intermodulation in RF MEMS variable capacitors," *IEEE Trans. Microw. Theory Tech.*, vol. 54, pp. 1120–1130, Mar. 2006.

[13] M. Innocent, P. Wambacq, S. Donnay, H. A. C. Tilmans, W. Sansen, and H. De Man, "An analytic Volterra-series-based model for a MEMS variable capacitor," *IEEE Trans. Comput.-Aided Design of Integr. Circuits Syst.*, vol. 22, pp. 124–131, Feb. 2003.

[14] J. Johnson, G. G. Adams, and N. E. McGruer, "Determination of intermodulation distortion in a MEMS microswitch," in *Proc. IEEE MTT-S Int. Symp. Digest*, Jun. 2005, pp. 2135–2138.

[15] A.-C. Wong and C. T.-C. Nguyen, "Micromechanical mixer-filters ("mixlers")," *IEEE J. Microelectromech. Syst.*, vol. 13, no. 1, pp. 100–112, Feb. 2004.

[16] A. T. Alastalo, M. Koskenvuori, H. Seppä, and J. Dekker, "A micromechanical resonating RF mixer," in *Proc. 34th Eur. Microw. Conf.*, Amsterdam, The Netherlands, Oct. 11 – 15, 2004, pp. 1297–1300.

[17] F. Chen, J. Brotz, U. Arslan, C.-C. Lo, T. Mukherjee, and G. K. Fedder, "CMOS-MEMS resonant RF mixer-filters," in *Proc. 18th IEEE Int. Conf. Micro Electro Mech. Syst.*, Miami, FL, Jan.-Feb. 30–3, 2005, pp. 24–27.

[18] A. Uranga, J. Verd, J. L. Lopez, J. Teva, G. Abadal, F. Torres, J. Esteve, F. Perez-Murano, and N. Barniol, "Fully integrated mixler based on VHF CMOS-MEMS clamped-clamped beam resonator," *IEE Electron. Lett.*, vol. 43, no. 8, pp. 452–454, Apr. 2007.

[19] G. M. Rebeiz*, RF MEMS, Theory, Design, and Technology*. New York: Wiley, 2003.

[20] C. Palego, S. Hadler, B. Baloglu, Z. Peng, J. C. M. Hwang, H. F. Nied, D. I. Forehand, and C. L. Goldsmith, "Microwave intermodulation technique for monitoring the mechanical stress in RF MEMS capacitive switches," in *Proc. IEEE MTT-S Int. Symp. Digest*, Jun. 15 – 20, 2008, pp. 29–32.

Ville V. Viikari (S'06–M'09) was born in Espoo, Finland, in 1979. He received the Master's of Science (Tech.), Licentiate of Science (Tech.) (with distinction), and Doctor of Science (Tech.) (with distinction) degrees in electrical engineering from the Helsinki University of Technology (TKK), Espoo, Finland, in 2004, 2006, and 2007, respectively.

From 2001 to 2007, he was a Trainee, Assistant Researcher, and Researcher with the Radio Laboratory, TKK, where he studied antenna measurement techniques at submillimeter wavelengths and antenna pattern correction techniques. He is currently a Research Scientist with the VTT Technical Research Centre, Espoo, Finland, and a Docent with TKK. His current research interests are RFID systems and wireless sensors.

Heikki Seppä was born in Kortesjärvi, Finland, in 1953. He received the Doctor of Science (Tech.) degree from the Helsinki University of Technology (TKK), Espoo, Finland, in 1989.

From 1976 to 1979, he was an Assistant at TKK, where he studied low-temperature physic and electrical metrology. In 1979, he joined the Technical Research Centre, Espoo, Finland, mainly to develop the quantum metrology. In 1989, he was appointed as a Research Professor at VTT. His research is focused on metrology, quantum devices, sensors, and specially on MEMS, wireless technology and nanotechnology. He worked several months at NIST USA (1982–1983) developing ultra low-temperature noise thermometer and in 2004, he was a Tutoring Professor in Nokia's Leading Science Program.

Authorized licensed use limited to: Valtion Teknillinen Tutkimuskeskus. Downloaded on November 26, 2009 at 05:25 from IEEE Xplore. Restrictions apply.